A Statistical Shape Model Approach for Computing Left Ventricle Volume and Ejection Fraction Using Multi-plane Ultrasound Images

Dawei Liu[1], Isabelle Peck[2], Shusil Dangi[1], Karl Q. Schwarz[3], and Cristian A. Linte[1(✉)]

[1] Rochester Institute of Technology, 1 Lomb Memorial Drive, Rochester, NY 14623, USA
{dxl1169,calbme}@rit.edu, shusil.dangi@gmail.com
[2] Rensselaer Polytechnic Institute, 110 8th Street, Troy, NY 12180, USA
pecki@rpi.edu
[3] University of Rochester Medical Center, 601 Elmwood Ave, Rochester, NY 14642, USA
karl_schwarz@urmc.rochester.edu

Abstract. Assessing the left ventricular ejection fraction (LVEF) accurately requires 3D volumetric data of the LV. Cardiologists either have no access to 3D ultrasound (US) systems or prefer to visually estimate LVEF based on 2D US images. To facilitate the consistent estimation of the end-diastolic and end-systolic blood pool volume and LVEF based on 3D data without extensive complicated manual input, we propose a statistical shape model (SSM) based on 13 key anchor points—the LV apex (1), mitral valve hinges (6), and the midpoints of the endocardial contours (6)—identified from the LV endocardial contour of the tri-plane 2D US images. We use principal component analysis (PCA) to identify the principle modes of variation needed to represent the LV shapes, which enables us to estimate an incoming LV as a linear combination of the principle components (PC). For a new, incoming patient image, its 13 anchor points are projected onto the PC space; its shape is compared to each LV shape in the SSM based on Mahalanobis distance, which is normalized with respect to the LV size, as well as direct vector distance (i.e., PCA distance), without any size normalization. These distances are used to determine the weight each training shape in the SSM contributes to the description of the new patient LV shape. Finally, the new patient's LV systolic and diastolic volumes are estimated as the weighted average of the training volumes in the SSM. To assess our proposed method, we compared the SSM-based estimates of diastolic, systolic, stroke volumes, and LVEF with those computed directly from 16 tri-plane 2D US imaging datasets using the GE Echo-Pac PC clinical platform. The estimated LVEF based on Mahalanobis distance and PCA distance were within 6.8% and 1.7% of the reference LVEF computed using the GE Echo-Pac PC clinical platform.

J. M. R. S. Tavares and R. M. Natal Jorge (Eds.): VipIMAGE 2019, LNCVB 34, pp. 540–550, 2019.
https://doi.org/10.1007/978-3-030-32040-9_55

1 Introduction

Left ventricular ejection fraction (LVEF) is a vital measure of the ventricular contraction efficiency that is calculated as a ratio of LV stroke volume and its volume at end-diastole. Despite its humble definition, LVEF is one of the most critical variables not just in cardiology, but across all disciplines of medicine. LVEF is used for daily management of cardiac patients, as well as a criterion for subject group divisions in research studies. Ultrasound (US) imaging is a standard-of-care, non-invasive method for imaging the heart in real time and is used to assess the left ventricle (LV) filling and ejection capabilities. Accurate estimation of the LV blood-pool volume entails the segmentation of the endocardial border of the LV from 3D US images. This process is challenging, time consuming, and susceptible to high inter- and even intra-user variability, since different clinicians perform the task based on varying empirical knowledge or habits. Moreover, to not compromise frame rate, cardiologists prefer to use multi-view 2D images as opposed to 3D images, the latter of which raises the need to reconstruct a 3D model of the LV blood pool from the several multi-plane 2D US images. As a current practice in clinical settings, cardiologists often visually estimate LVEF based on the area changes of the blood pool as viewed in the real-time 2D US images of the heart. In our previous work [6,7], we demonstrated that the LVEF estimates based on area changes significantly underestimate the true LVEF computed based on volume changes, by as much as 13%. Therefore, an efficient method to calculate the true LVEF based on volume changes that minimize manual interaction to reduce inter- and intra-user variability is paramount.

Left ventricles can have innumerable shapes that pose challenges for developing a comprehensive model to encompass the variations in their geometries. A few geometric models such as cylindrical [4], truncated prolate spheroid [3], and paraboloid [15] were published to mathematically describe an LV shape, but they are not sufficiently accurate to represent patient-specific anatomy. Statistical shape models (SSMs) have been employed by several researchers in the field of cardiology to capture the characteristics of LV shapes and endocardial wall motion from a population of subjects. Previous works mainly focused on identifying characteristics of LV morphological changes associated with cardiac disease or treatment [1,5,8]. Generally, LV geometric coordinates are defined and assembled into a statistical model that comprises all of the coordinates in the population. A mean shape is then generated and the deviation from an individual LV geometry to the mean geometry is calculated. In multiple studies, researchers successfully distinguished LV shapes associated with cardiac disease or surgical intervention from healthy LV shapes. Moreover, SSM led to accuracies in the range of 83% to 98% when used to classify LV geometric morphology [12]. Due to the usually large number of modes of variation, multiple attempts [1,5,9,11,13,14] were made to reduce and analyze the modes of variation in SSM by using principle component analysis (PCA). Several researches discovered that the first three to five principle components calculated from PCA explain the majority of geometric variances such as size, sphericity, and concentricity [8,10].

Hence, SSMs constitute a promising method to characterize LV shapes even with a wide range of variability, this method shall enable us to efficiently estimate LV volumes with or without size effect.

Here we propose a method that relies on a SSM generated using a population of retrospective patient-specific cardiac US images. In compliance with Health Insurance Portability and Accountability Act (HIPPA) regulation, all patient information were de-identified. The SSM uses tri-plane 2D US images depicting the heart at both systole and diastole from 66 patients. In each tomographic view of the tri-plane images, five anchor points were identified by the user. Since one of the five anchor points is the apex of the LV, it co-exists at the same location in all three tomographic views, therefore leading to the LV endocardial shape representation consisting of 13 anchor points: the LV apex (1), mitral valve hinges (6), and the midpoints of the endocardial contours (6).

A ground truth segmentation of the blood pool, along with end-systolic and diastolic volumes, stroke volume, and LVEF computed using the GE Echo-Pac PC standard-of-care clinical platform were available for each dataset and served as gold standard metrics against which our methods were assessed. Once the SSM was generated from 50 of the 66 datasets, it is used to estimate the systolic volumes, diastolic volumes, and their corresponding LVEFs for the remaining 16 testing datasets. The estimated values were then compared to the ground truth values.

In this paper, we describe the construction of the SSM and demonstrate its feasibility to estimate blood pool volume and LVEF, assess their accuracy versus the ground truths, and further support the hypothesis that the estimated LVEF based on true volume measurement is more faithful than area-based LVEF estimate.

2 Methodology

2.1 Patient Data and Anchor Points

The first task of this project was to manually obtain the 13 anchor points for each tri-plane image dataset. In each tri-plane image dataset for each of the 66 patients, there were three images corresponding to three tomographic views of the LV acquired at roughly 60° apart: the 2-chamber view, 3-chamber view (or, sometimes, parasternal long-axis view (PLAX) view), and 4-chamber view. For each tomographic view in the tri-plane image set, five anchor points were selected by the user. The five anchor points are located at five landmarks of the LV endocardial border: apex, mitral valve hinges, and midpoints of the endocardial wall on each side. The LV apex remains stationary during a cardiac cycle, so only one unique set of coordinates exists for the apex in all three views, which resulted in a total of 13 anchor points describing each dataset. Of the 66 patient-specific image datasets in total, 50 were used as the training data for the SSM and the remaining 16 were used as testing data. The shapes characterized by the 13 anchor points, method of disc (MOD) volumes, and 3D reconstructed

volumes of the 50 training data were used to predict the volumes and LVEFs of the 16 test datasets (Fig. 1).

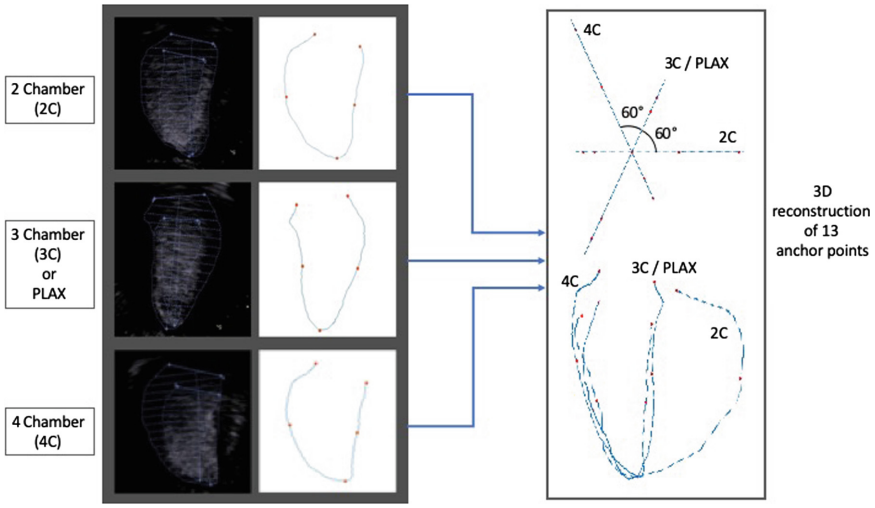

Fig. 1. Anchor point locations on an example diastolic LV endocardial border (the outer-most blue trace in the images with black background in the left column).

The 3D LV blood pool geometry of each patient consisted of a set of 13 anchor landmarks in systole and the same in diastole, while the SSM LV geometry consisted of 50×13 anchor landmarks in systole and same in diastole. Even though the anchor points were selected from 2D images, their transposition into the corresponding 3D volume was obtained under the clinically supported premise that the tri-plane 2D images were collected at 60° apart. Using a reconstruction algorithm previously developed and validated in our earlier work [2], all 2D anchor points were transformed into the 3D space, resulting in the SSM of dimension $50 \times 13 \times 3$ (Fig. 2).

2.2 LV Volume Estimation via Size Normalization and Mahalanobis Distance

Once the SSM was generated, it was used to estimate the systolic and diastolic volumes of an incoming test patient. We used the inverse co-variance matrix of the SSM to calculate the Mahalanobis distance between the test data and each of the training data in the SSM. The Mahalanobis distance can be calculated as defined below:

$$d_i = (test - train_i)^T C^{-1} (test - train_i), \tag{1}$$

where d_i is the Mahalanobis distance between a test data and each of the 50 training data with an index of i, C^{-1} is the inverse co-variance matrix of the SSM,

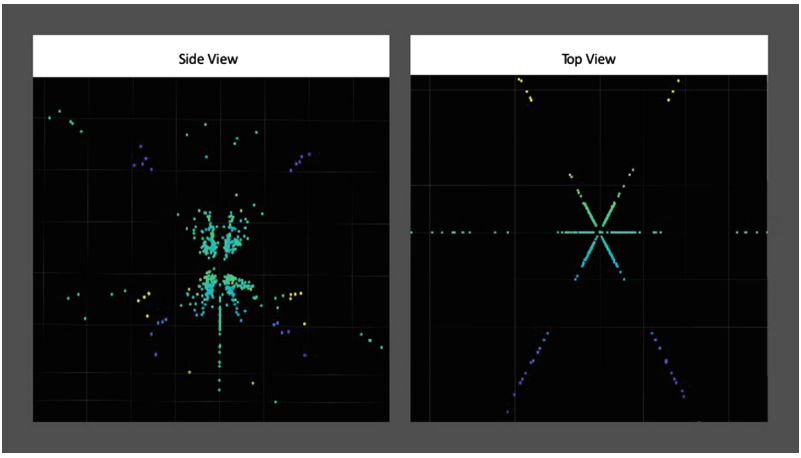

Fig. 2. The point cloud constructed based on 13 anchor points from each of the 50 training datasets.

and $()^T$ is the matrix transpose operation. The Euclidean distance $(test - train_i)$ between testing and training data in 3D space is calculated first, and its transpose is then multiplied by the co-variance matrix of the SSM, as well as the Euclidean distance.

The Mahalanobis distance between the test and each training data is used to calculate the weight according to which each training dataset contributes to the description of a new dataset. These weights were, in turn, used to estimate the systolic and diastolic volumes of the test data.

$$w_i = \frac{\sum_{i=0}^{50} d_i}{d_i} \tag{2}$$

Finally, either both systolic or diastolic volume of the test data can be estimated using the calculated weights multiplied by the corresponding ground truth volumes of each training dataset.

$$V_{estimated} = \sum_{i=0}^{50} w_i V_i \tag{3}$$

The ground truth LV volumes were calculated by method of disc (MOD) that were generated by the standard-of-care platform—GE EchoPac PC—used by our collaborator to acquire the patient-specific US tri-plane images. On each US image acquired and analyzed using EchoPac, there is a legend box that details the MOD volumes for the systolic and diastolic blood pools. The systolic or diastolic MOD volumes were automatically calculated by the EchoPac by averaging the volumes estimated from the three tomographic views of a patient's LV to obtain a single systolic or diastolic volume. Hence, the average MOD volume is defined by the following equation (Fig. 3).

$$V_{MOD/average} = \frac{V_{MOD/2C} + V_{MOD/3C(PLAX)} + V_{MOD/4C}}{3}. \quad (4)$$

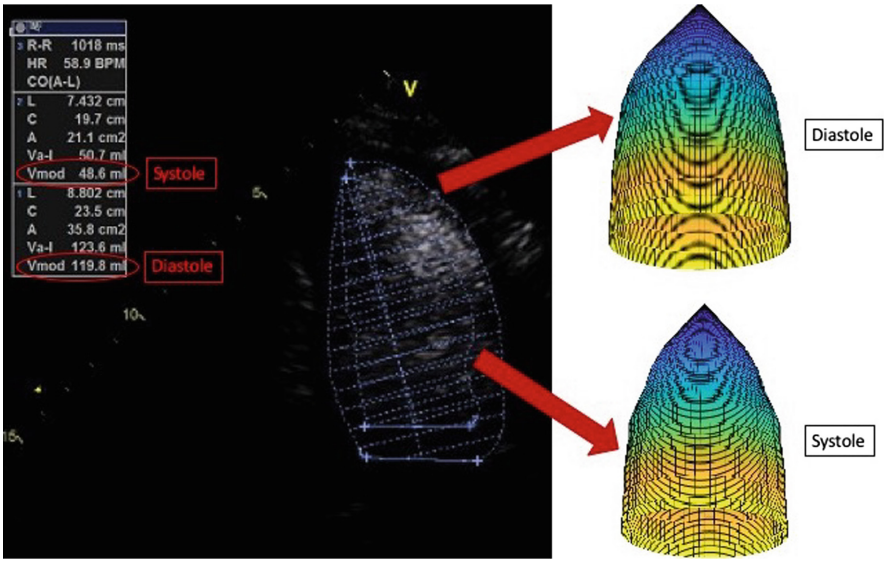

Fig. 3. An example US image captured on GE EchoPac PC with legend showing systolic and diastolic volumes using MOD algorithm, which assumes the LV volume is axisymmetric, as the simulated model shown in the right image panel.

2.3 LV Volume Estimation via Vector Distance Without Size Normalization

As opposed to using the Mahalanobis distance which removes the effect of size differences in the LV shape, we also employed an alternative, yet more traditional method to account for the size effect. The vector distance resulting from the dot product of the test patient's anchor points and each training patient's anchor points was used to determine the contributing weight of each training LV shape in the SSM for test patient LV volume estimations. To assist with PCA in the later steps, the matrix containing all 50 training patients' 3D anchor points was first reshaped from $50 \times 13 \times 3$ to 50×39.

$$A = 50 \times \begin{bmatrix} x_1 & y_1 & z_1 \\ x_2 & y_2 & z_2 \\ \vdots & \vdots & \vdots \\ x_1 3 & y 13 & z_1 3 \end{bmatrix} \Rightarrow 50 \times \begin{bmatrix} x_1 \\ y_1 \\ z_1 \\ x_2 \\ y_2 \\ z_2 \\ \vdots \\ x_{13} \\ y_{13} \\ z_{13} \end{bmatrix} \tag{5}$$

Since obtaining real eigenvalues and eigenvectors requires the training patient anchor point matrix to be a symmetric matrix, we first computed the Gramian matrix as follows:

$$A' = [50 \times 39]^T [50 \times 39] = [39 \times 50] [50 \times 39] = [39 \times 39] . \tag{6}$$

By performing the eigen-decomposition of the training patient anchor point matrix, the eigenvalues and eigenvectors were calculated. The eigenvalues were sorted in descending order, and the eigenvectors were sorted correspondingly. The training and test patient anchor points were projected onto PCA space via multiplication by the eigenvector matrix, enabling the representation of each LV shape in terms of the 39 modes of variation identified via eigen-decomposition. Finally, the vector distance in PCA space between a test patient's anchor points and training patient's anchor points was calculated using the dot product operation. The vector distance was used as the weight according to which each training patient's diastolic and systolic volumes contribute to describing a test patient's corresponding volumes, similar to Eq. 3. Following this process, the systolic and diastolic volumes of all 16 test patients were estimated.

3 Results and Discussion

Table 1 summarizes the results for the estimated blood pool volumes and LVEFs based on Mahalanobis distance (Estimate 1) and vector distance (Estimate 2), versus their corresponding ground truth values. As shown, both SSM-based estimates were within 6.8% and 1.7% of the ground truth.

Examining the average systolic and diastolic volumes for the test data, the results are determined to be reasonable. The Estimate 1 (i.e., Mahalanobis distance following size normalization) results are lower than ground truth, overall, due to the contribution of some of the smaller volumes in the training data in the SSM. This trend can potentially be corrected by only using the several highest contributing modes of variation identified across all 50 training datasets to describe a new, incoming LV shape, instead of using all 39 modes of variation. Estimate 2 (i.e., vector distance without size normalization) results are much closer to the ground truth data, indicating that the size of LV shapes is a major

mode of variation to be considered, and hence size normalization (i.e., Estimate 1) may fail to capture the proper size effect. The mean and standard deviations of the ground truth as well as estimated systolic and diastolic volumes and LVEF are summarized in Table 1.

Table 1. Comparison of LVEFs, diastolic volumes, and systolic volumes from the reference image data, estimation method 1, and estimation method 2.

Mean ± Std. Error[a]	Image data	Estimate 1	Estimate 2
LVEF [%]	55.7 ± 4.7	48.9 ± 4.3	57.4 ± 5.0
Diastolic volume [ml]	125.8 ± 17.9	117.3 ± 17.4	126.8 ± 18.1
Systolic volume [ml]	66.4 ± 17.7	68.7 ± 16.9	66.9 ± 17.9

[a] $Standard\ Error = Standard\ Deviation\ /\ \sqrt{Number of Samples}$

As an additional visual aide to analyze the results, the LVEF, diastolic volume, and systolic volume of all 16 test patient from reference image data, Estimate 1, and Estimate 2 are shown in Figs. 4 and 5 as box and whisker plots. The black 'X' symbols show the means of each data type. The gray boxes illustrate the range between the median and third quartile and the orange boxes illustrate the range between the median and the first quartile. The top whiskers illustrate the range between the third quartile to the maximums and the bottom whiskers illustrate the range between the first quartile to the minimums. The results from Estimate 1 and Estimate 2 are reasonably close to the ground truth image data.

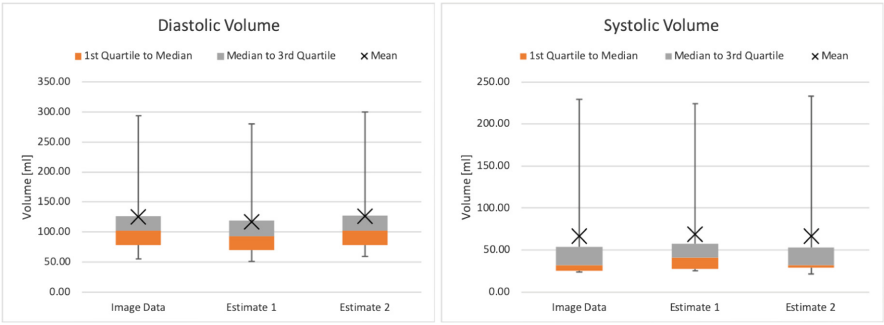

Fig. 4. Reference and estimated diastolic and systolic volumes based on MOD applied to image data, Mahalanobis distance (Estimate 1), and vector distance (Estimate 2).

As shown in Table 2, following an ANOVA comparison between the ground truth data, Estimate 1 and Estimate 2 data, the p-values are all higher than 0.05 and F values are all lower than the critical F values for diastolic volume, systolic volume, and LVEF, hence suggesting no statistically significant difference between the ground truth parameters and those estimated using the proposed SSM method.

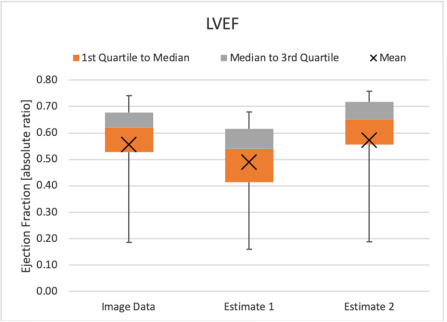

Fig. 5. Reference and estimated LVEFs based on MOD applied to image data, Mahalanobis distance (Estimate 1), and vector distance (Estimate 2).

Table 2. One-way ANOVA tests of LVEFs, diastolic volumes, and systolic volumes from the reference image data, estimation method 1, and estimation method 2.

Quantity	P-value	F value	F critical
LVEF	0.41	0.92	3.20
Diastolic volume	0.92	0.09	3.20
Systolic volume	0.99	0.01	3.20

4 Conclusion and Future Work

We described a method to estimate diastolic and systolic volumes, and LVEF using select key landmarks on the LV endocardial borders and a pre-trained SSM. This approach provides a viable means for quickly and accurately estimating the blood pool volume and LVEF with minimal manual interaction using volume rather than area-based measurements. This method enables clinicians to select only a few endocardial anchor points from the multi-plane 2D US images to estimate the 3D volume and LVEF and provides meaningful progress toward preventing crude visual estimations, often employed in current practice. Lastly, our study showed no statistically significant differences between the ground truth volume and LVEF parameters (obtained using the GE Echp-Pac PC clinical platform) and the corresponding parameters estimated using our proposed SSM-based approach. These estimates may be further improved with additional training data.

As part of our future work, we will also assess our SSM-based estimates against the same parameters computed using native 3D US data, which will also help assess whether the axisymmetric MOD estimates of the LV blood pool provided by the GE EchoPac PC platform is truly a sufficiently viable and accurate metric.

Acknowledgements. This work was supported by the National Institutes of Health under Award No. R35GM128877 and by the National Science Foundation under Award No. 1808530.

References

1. Bruse, J.L., Ntsinjana, H., Capelli, C., Biglino, G., McLeod, K., Sermesant, M., Pennec, X., Hsia, T.Y., Schievano, S., Taylor, A.: CMR-based 3D statistical shape modelling reveals left ventricular morphological differences between healthy controls and arterial switch operation survivors. J. Cardiovasc. Magn. Reson. **18** (2016)
2. Dangi, S., Ben-Zikri, Y.K., Cahill, N., Schwarz, K.Q., Linte, C.A.: Endocardial left ventricle feature tracking and reconstruction from tri-plane trans-esophageal echocardiography data. In: Medical Imaging 2015: Image-Guided Procedures, Robotic Interventions, and Modeling, vol. 9415, p 941505 (2015)
3. Domingues, J.S., Vale, M.D.P., Martinez, C.B.: New mathematical model for the surface area of the left ventricle by the truncated prolate spheroid. Sci. World J. **2017**, 6981515 (2017)
4. Dumesnil, J., Shoucri, R., Laurenceau, J., Turcot, J.: A mathematical model of the dynamic geometry of the intact left ventricle and its application to clinical data. Circulation **59**, 1024–1034 (1979). https://doi.org/10.1161/01.cir.59.5.1024
5. Farrar, G., Suinesiaputra, A., Gilbert, K., Perry, J.C., Hegde, S., Marsden, A., Young, A.A., Omens, J.H., McCulloch, A.D.: Atlas-based ventricular shape analysis for understanding congenital heart disease. Prog. Pediatr. Cardiol. **43**, 61–9 (2016)
6. Liu, D., Peck, I., Dangi, S., Schwarz, K., Linte, C.: Left ventricular ejection fraction: comparison between true volume-based measurements and area-based estimates. In: 2018 IEEE Western New York Image and Signal Processing Workshop (WNYISPW), pp. 1–5 (2018)
7. Liu, D., Peck, I., Dangi, S., Schwarz, K., Linte, C.: Left ventricular ejection fraction assessment: unraveling the bias between area- and volume-based estimates. In: Proceedings SPIE Medical Imaging - Ultrasonic Imaging and Tomography, vol. 10955, pp. 109550T–1–8 (2019)
8. Medrano-Gracia, P., Cowan, B.R., Ambale-Venkatesh, B., Bluemke, D.A., Eng, J., Finn, J.P., Fonseca, C.G., Lima, J.A., Suinesiaputra, A., Young, A.A.: Left-ventricular shape variation in asymptomatic populations: the multi-ethnic study of atherosclerosis. J. Cardiovasc. Magn. Reson. **16**, 56 (2014). https://doi.org/10.1186/s12968-014-0056-2
9. Medrano-Gracia, P., Cowan, B.R., Finn, J.P., Fonseca, C.G., Kadish, A.H., Lee, D.C., Tao, W., Young, A.A.: The cardiac atlas project: preliminary description of heart shape in patients with myocardial infarction. In: Camara, O., Pop, M., Rhode, K., Sermesant, M., Smith, N., Young, A. (eds.) Statistical Atlases and Computational Models of the Heart, pp. 46–53 (2010)
10. Piras, P., Teresi, L., Puddu, P., Concetta, T., Young, A., Suinesiaputra, A., Medrano-Gracia, P.: Morphologically normalized left ventricular motion indicators from MRI feature tracking characterize myocardial infarction. Sci. Rep. **7** (2017)
11. Remme, E.W., Young, A.A., Augenstein, K.F., Cowan, B., Hunter, P.J.: Extraction and quantification of left ventricular deformation modes. IEEE Trans. Biomed. Eng. **51**, 1923–31 (2004)

12. Suinesiaputra, A., Ablin, P., Albà, X., Alessandrini, M., Allen, J., Bai, W., Cimen, S., Claes, P., Cowan, B., D'hooge, J., Duchateau, N., Ehrhardt, J., Frangi, A., Gooya, A., Grau, V., Lekadir, K., Lu, A., Mukhopadhyay, A., Oksuz, I., Medrano-Gracia, P.: Statistical shape modeling of the left ventricle: myocardial infarct classification challenge. IEEE J. Biomed. Health Inform. **22**, 503–15 (2017)
13. Tejman-Yarden, S., Bratincsak, A., Bachner-Hinenzon, N., Khamis, H., Rzasa, C., Adam, D., Printz, B.F., Perry, J.C.: Left ventricular mechanical property changes during acute av synchronous right ventricular pacing in children. Pediatr. Cardiol. **37**, 106–111 (2016)
14. Zhang, X., Cowan, B.R., Bluemke, D.A., Finn, J.P., Fonseca, C.G., Kadish, A.H., Lee, D.C., Lima, J.A.C., Suinesiaputra, A., Young, A.A., Medrano-Gracia, P.: Atlas-based quantification of cardiac remodeling due to myocardial infarction. PLOS ONE **9**(10), 1–13 (2014)
15. Zhong, L., Su, Y., Yeo, S.Y., Tan, R.S., Ghista, D.N., Kassab, G.: Left ventricular regional wall curvedness and wall stress in patients with ischemic dilated cardiomyopathy. Am. J. Physiol.-Heart Circu. Physiol. **296**, H573–84 (2009)